

Optical properties of amorphous $\text{As}_{45}\text{S}_{15}\text{Se}_{40}$ thin films

M. S. IOVU*, I. A. COJOCARU, V. G. BENEĂ, E. P. COLOMEICO

Institute of Applied Physics, Academy of Sciences of Moldova, Str. Academiei 5, MD-2028, Chisinau, R. Moldova

The experimental investigations of the influence of the light irradiation on the optical parameters of one of highest sensitive chalcogenide glass $[(\text{As}_{40}\text{S}_{60})_{0.5}:(\text{As}_{40}\text{Se}_{60})_{0.5}]_{0.5}:(\text{As}_{50}\text{Se}_{50})_{1.0}$ was investigated. For the amorphous $\text{As}_{45}\text{S}_{15}\text{Se}_{40}$ thin films, prepared by „flash” thermal evaporation, from the transmission spectra the value of the refractive index n was found $n=2.921$ at $\lambda=650$ nm, and the optical band gap E_g was determined from the Tauc plot $E_g=1.929$ eV. The kinetics of photodarkening in amorphous $\text{As}_{45}\text{S}_{15}\text{Se}_{40}$ thin films is described by stretch exponential function and the effect at illumination with laser beam $\lambda=540$ nm is more pronounced than in amorphous As_2S_3 and As_2Se_3 films. The maximum of the diffraction efficiency η of the holographic gratings recorded during the exposure of laser beam at $\lambda=540$ nm is reached at about $t=250$ s.

(Received May 5, 2011; accepted November 23, 2011)

Keywords: Chalcogenide glass, amorphous films, optical transmission, holography

1. Introduction

Amorphous As_2S_3 , As_2Se_3 and $\text{As}_2\text{S}_3\text{-As}_2\text{Se}_3$ have been intensively studied as promising materials for recording media and different methods have been applied to fabricate diffractive optical elements using holographic or electron beam lithography methods [1,2]. The physical principles of these methods are based on the effect of photoinduced phenomena in chalcogenide glasses, e.g. the changes of the optical constants (absorption coefficient α , optical band gap E_g , and refractive index n) of the material under the ionization irradiation. It was demonstrated, that in amorphous As_2S_3 thin films can be recorded can be recorded the transmission holographic gratings with the diffraction efficiency up to $\eta=80$ % [3]. For the amorphous $\text{As}_{100-x}\text{Se}_x$ films the maximum photoinduced refractive index ($\Delta n=0.73$) [3] and ($\Delta n/n=0.394$) [4] changes was observed for the glass composition $\text{As}_{60}\text{Se}_{40}$. The surface relief holographic gratings with the period $A=0.15\div 1$ μm in amorphous As_2S_3 and $\text{As}_{40}\text{S}_{15}\text{Se}_{45}$ thin films were recorded using the solid immersion holographic method (using prisms from ZnS or GaP with a refractive index of $n=3$ or more) [1,5]. The photoinduced changes in vacuum evaporated amorphous $\text{As}_2\text{S}_3\text{-As}_2\text{Se}_3$ thin films in the infrared absorption spectra are interpreted by rearrangement (polymerization) of bonding configurations (Such molecular units as As_4 , As_4S_3 , As_4S_4 , S_8 , As_4Se_4 , etc.) [6]. It was shown that after irradiation of the as-deposited amorphous films the IR spectrum becomes similar to that of a thermally annealed sample, similar to that of a bulk material. In order to explain the role of S/Se ratio in As-S-Se glasses, was investigated different glasses using Raman spectroscopy, x-ray photoelectron spectroscopy (XPS), and extended x-ray absorption fine structure spectroscopy (EXAFS), and compared with the stoichiometric compositions $\text{As}_{40}\text{S}_{60}$ and $\text{As}_{40}\text{Se}_{60}$ [7]. It was demonstrated that the molecular structure of the

mixed glasses is similar to the binary glasses and consists of a network of chalcogen chain fragments cross-linked by pyramidal AsCh_3 units. At the same time the presence of the substantial amount of S-S, S-Se, Se-Se, As-As and S_8 rings are possible. For the amorphous $\text{As}_{40}\text{Se}_{60-x}\text{Se}_x$ thin films was established that increasing of Se concentration leads to increasing of the refractive index [8]. The exposure and annealing lead to polymerization of the molecular groups As_4S_4 and As_4Se_4 and the chains S_n and Se_n in the film matrix, with further formation of structural units characterized with heteropolar As-S and As-Se bonds. The latter is accompanied by the shift of the absorption edge towards the long wavelength region and the increasing of the refractive index. In the present work we present the experimental investigations of the influence of the light irradiation and thermal annealing on the optical parameters of one of highest sensitive chalcogenide glass $[(\text{As}_{40}\text{S}_{60})_{0.5}:(\text{As}_{40}\text{Se}_{60})_{0.5}]_{0.5}:(\text{As}_{50}\text{Se}_{50})_{1.0}$ (the short formula $\text{As}_{45}\text{S}_{15}\text{Se}_{40}$). It is expected that adding of As_5Se_5 to the glass composition $(\text{As}_2\text{S}_3)_{0.5}:(\text{As}_2\text{Se}_3)_{0.5}$ (or $\text{As}_{40}\text{S}_{30}\text{Se}_{30}$) will provide the shift of the absorption edge in the longer wavelength, increase the refractive index and the photoinduced changes of the refractive index. The optical constants (absorption coefficient α , optical band gap E_g , and the refractive index n) were calculated from the experimental measured transmission spectra. The kinetics of photodarkening in amorphous $\text{As}_{45}\text{S}_{15}\text{Se}_{40}$ thin films also was investigated and interpreted in framework of the existing models for photodarkening in amorphous semiconductors.

2. Experimental

The bulk samples of chalcogenide glasses $[(\text{As}_{40}\text{S}_{60})_{0.5}:(\text{As}_{40}\text{Se}_{60})_{0.5}]_{0.5}:(\text{As}_{50}\text{Se}_{50})_{1.0}$ was synthesized from the mixture of the preliminary prepared

(As₄₀S₆₀)_{0.5}:(As₄₀Se₆₀)_{0.5} and As₅₀Se₅₀ glasses. The mixture of high-purity precursors was melted in sealed evacuated quartz ampoules ($p=5 \cdot 10^{-6}$ Torr) placed in a rocking furnace. The total weight of the synthesized sample was 50 grams. The temperature of the quartz ampoule was slowly increased to 550 °C at the rate of 50 °C/hour and kept at this temperature during 24 hours for homogenization. Then the temperature was increased up to 980 °C at the rate 50 °C/hour and homogenized at this temperature during 72 hours, and then quenched in the regime of the disconnected furnace.

Thin film samples of thickness $d=0.5 \div 3$ μm were prepared by flash thermal evaporation in vacuum of the synthesized initial chalcogenide glass onto glass substrates held at $T_{subs}=100$ °C. For optical transmission spectra measurements a UV/VIS ($\lambda=300 \div 800$ nm) and 61 NIR ($\lambda=800 \div 3500$ nm) Specord's CARLZEISS Jena production were used. For calculation of the optical constants from the transmission spectra, the computer program *PARAV-V1.0* (www.chalcogenide.eu.org) was used [9]. To initiate photostructural transformations in thin film samples, as a source of light exposure, a continuous He-Ne lasers ($\lambda=630$ nm, $P=0.6$ mW and $\lambda=543$ nm, $P=0.75$ mW) were used. The experimental set-up included a laser, a digital build-in PC-card *PCI-1713A* for data acquisition connected with the *Si*-photodetector. The transmission holographic gratings were recorded by two symmetrically incident laser beams ($\lambda=543$ nm, $\theta \sim 15^\circ$) of equal intensity. The diffraction efficiency η is defined as $\eta = I_d/I_0$, where I_0 is the intensity of the incident beam, I_d is the intensity of the first order diffracted beam.

3. Results and discussion

Fig. 1 represents the typical transmission spectra for amorphous As₄₅S₁₅Se₄₀ thin film sample. From the transmission spectra $T=f(\lambda)$, using the expressions

$$\alpha = \frac{1}{d} \ln \frac{(1-R)^2}{T}, \quad n = \frac{\lambda_m \lambda_{m-1}}{2d(\lambda_{m-1} - \lambda_m)}$$

and the dependence $(\alpha h\nu)^{1/2} = A(h\nu - E_g)$, was calculated the absorption coefficient α , the refractive index n , and the value of the optical band gap E_g respectively. Here d – is the thickness of the sample, R – the reflection, λ_m, λ_{m-1} – the minimum and maximum of the interference in the transmission spectra, A – is a constant.

The computing fitting of the dependence $(\alpha h\nu)^{1/2} = A(h\nu - E_g)$ and the extrapolation of the Urbach tail to zero give the value of the optical band gap $E_g=1.929$ eV. Fig.2 represents the dispersion curve $n=f(\lambda)$ amorphous As₄₅S₁₅Se₄₀ thin film ($d=2.4$ μm). With increasing the wavelength the value of the refractive index n decrease at $\lambda \sim 700$ nm reach the saturation.

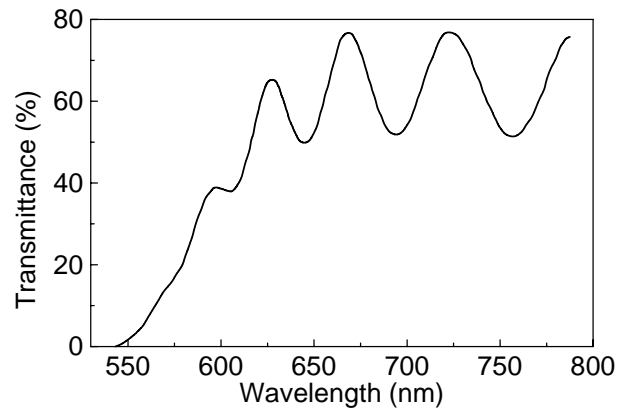


Fig.1. The transmission spectra of amorphous As₄₅S₁₅Se₄₀ thin film ($d=2.4$ μm).

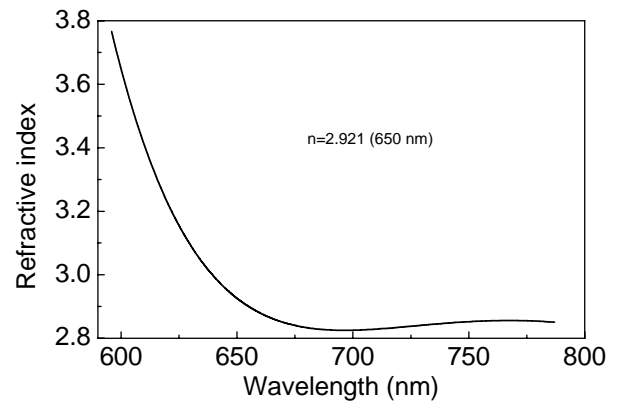


Fig.2. The dispersion curve $n=f(\lambda)$ for amorphous As₄₅S₁₅Se₄₀ thin film ($d=2.4$ μm).

Some optical properties and photoinduced phenomena of amorphous films from the As-S-Se glassy system were investigated by Raman spectroscopy [6-8]. In the present paper we present the influence of the exposure time and the annealing temperature on the optical constants (optical band gap E_g and refractive index n) of amorphous As₄₅S₁₅Se₄₀ thin films. Fig.3 represents the dependence of the optical band gap E_g and refractive index n versus the exposure time t_{exp} for amorphous As₄₅S₁₅Se₄₀ thin films. Increasing of the exposure time decrease the value of the optical band gap E_g , while the value of the refractive index n increase. Increasing of the refractive index n for exposed and annealed amorphous As₄₀S_{60-x}Se_x films was observed in [8], and was explained by polymerization of the molecular groups As₄S₄ and As₄Se₄ and the chains S_n and Se_n in the film matrix, with further formation of structural units characterized with heteropolar As-S and As-Se bonds. These features of the molecular structure of Chalcogenide amorphous films also leads to decreasing of the optical band gap during illumination and annealing (Fig.3 and Fig.4).

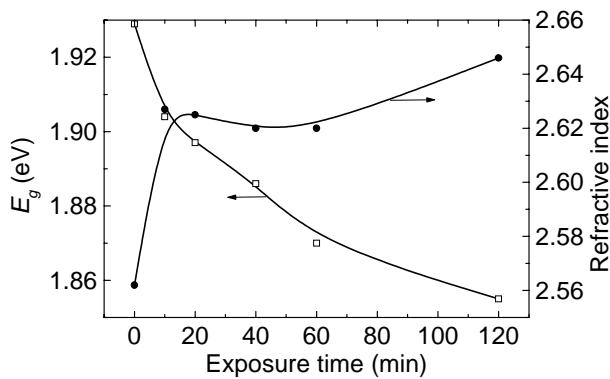


Fig. 3. The dependence of the optical band gap E_g and refractive index n versus the exposure time t_{exp} for amorphous $As_{45}S_{15}Se_{40}$ thin films.

According to [10], the shift of the band gap $\Delta E_g(t)$ versus time of illumination for amorphous $Ge_5As_{41}S_{15}Se_{39}$ films can be describe by the relation $\Delta E_g(t) = \Delta E_{g\infty}(1 - \exp[-(kt)^\beta])$, where $\Delta E_{g\infty} = E_g(t \rightarrow \infty) - E_g$, k is the formal rate constant of the overall process, t is the time of illumination and β is so called stretching parameter. For different processes (illumination with sub-gap light, with over-band light and with white light) were obtained different dependences. In our case this dependence $\Delta E_g(t)$ also can be approximate with stretch exponential. On the other hand, the dependences of the optical band gap ΔE_g and refractive index n versus annealed temperature T_{ann} , up to $T_{ann} = 100$ °C are almost linearly (Fig.4). For amorphous $As_{45}S_{15}Se_{40}$ thin films these coefficients, approximated from the dashed lines in Fig.4 took the values; $\Delta E_g/\Delta T_{ann} = -5.8 \cdot 10^{-4}$ eV/°C, and $\Delta n/\Delta T_{ann} = -9.2 \cdot 10^{-4}$ 1/°C, respectively.

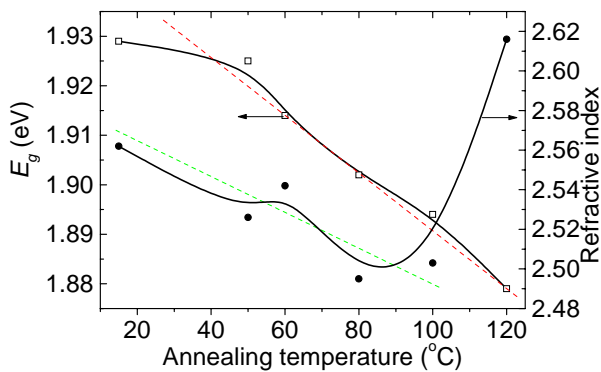


Fig.4. The dependence of the optical band gap E_g and refractive index n versus the annealing temperature T_{ann} for amorphous $As_{45}S_{15}Se_{40}$ thin films.

The relaxation of the relative optical transmission for some amorphous $As_{45}S_{15}Se_{40}$ thin film thin films in the coordinates $T(t)/T(0)$ vs t is shown in Fig.5 (curve 1), when excited with He-Ne laser ($\lambda = 540$ nm). For comparison in the Fig.5 also are presented the photodarkening process for amorphous As_2Se_3 (curve 2) and As_2S_3 (curve 3) thin

films. From Fig.4 it is seen that the amorphous $As_{45}S_{15}Se_{40}$ thin film exhibits the stronger photodarkening effect, e.g. are more sensitive to the light exposure. These dependences describe the excess of absorbance induced by light absorption during the time exposure. At a constant light intensity the presented dependences characterize the decay of the film optical transmittance with the increase of the dose of absorbed photons. To obtain a unified basis for comparison of the transmission relaxation $T(t)/T(0)$ curves we used so called stretched exponential presentation for the relaxation curves in the form:

$$T(t)/T(0) = A_0 + A \exp[-(t-t_0)/\tau]^{(1-\beta)},$$

t is the exposure time, τ is the apparent time constant, $A = I - A_0$ characterizes the “steady-state” optical losses due to photodarkening, t_0 and A_0 are the initial coordinates, and β is the dispersion parameter ($0 < \beta < 1$). Parameters of the stretched exponential obtained by fitting of the experimental points and calculated curves for amorphous $As_{45}S_{15}Se_{40}$ thin films are presented in the insert of Fig.5.

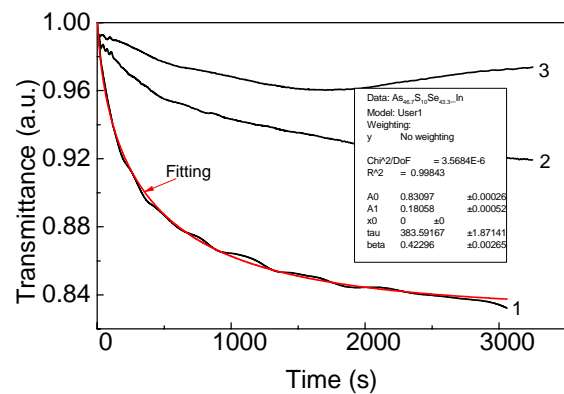


Fig.5. The kinetics of photodarkening in amorphous $As_{45}S_{15}Se_{40}$ (curve 1), As_2Se_3 (curve 2), and As_2S_3 (curve 3) thin films.

The high photoinduced changes of the refractive index $\Delta n = 0.1 \div 0.5$ in amorphous films of chalcogenide glasses make it promising materials for holographic recording media with high density [3,5,11-13]. These particularities permit to use the amorphous layers from chalcogenide glasses for fabrication of diffraction gratings, channel waveguides, and other diffractive elements for integrated optics. The microholograms were recorded as result of interference of two He-Ne laser beams ($\lambda = 543$ nm) with a power of $W = 0.75$ mW. Fig. 6 shows the kinetics growth of the diffraction efficiency versus recording time for amorphous As_2Se_3 (curve 1), two-layer structure As_2Se_3/As_2S_3 (curve 2), and $As_{45}S_{15}Se_{40}$ (curve 3) thin films. It is observed, that the maximum diffraction efficiency was obtained for amorphous $As_{45}S_{15}Se_{40}$ thin films, and after the maximum the curve fall down slowly than in the other two amorphous structures. The analogical

shape of the curves with the maximum was observed earlier for different amorphous materials [5,11-13].

The intensity of the first interference maximum was recorded in the transmittance mode. The maximum of the diffraction efficiency is reached at recorded times $t=3\div 5$ min of the exposure. The results regarding the sensitivity and the values of the diffraction efficiency for different amorphous films correlate with that obtained on photodarkening (Fig.5).

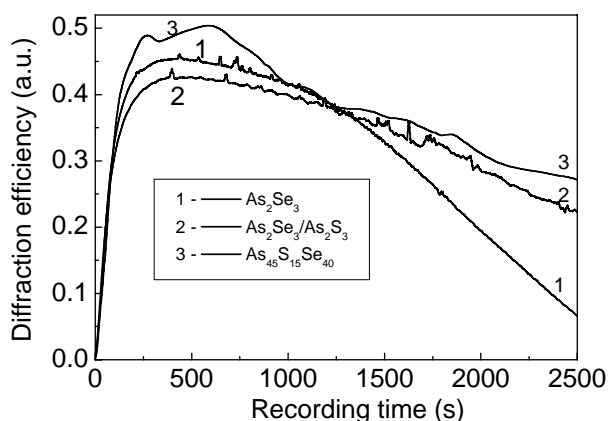


Fig. 6. The kinetics growth of the diffraction efficiency versus recording time for amorphous As_2Se_3 (curve 1), two-layer structure $\text{As}_2\text{Se}_3/\text{As}_2\text{S}_3$ (curve 2), and $\text{As}_{45}\text{S}_{15}\text{Se}_{40}$ (curve 3) thin films.

The investigations on modification of the refractive index under the illumination and the holographic recording process in the amorphous films of $\text{As}_x\text{S}_{1-x}$ and $\text{As}_x\text{Se}_{1-x}$, and As-S-Se systems [3,12] show that the more sensitive are the glasses with rich content of Arsenic. This fact also is demonstrated in the experiments on photodarkening (Fig.), where for the composition $\text{As}_{45}\text{S}_{15}\text{Se}_{40}$ (curve 1) we have obtained more pronounced effect, that in the stoichiometric compositions of As_2Se_3 (curve 2), and As_2S_3 (curve 3). The fact that the photodarkening kinetics may be described by a stretched exponential we may consider as indication of dispersion in kinetic mechanism, i.e. the time dependence of the process rate. The data allow concluding that formation of photoinduced absorption is limited by a dispersive process with the exponent $\beta \cong 0.4\div 0.5$. In our case it is the dispersive character of hole transport that may cause the dispersive character of the relaxation after photogeneration. The transport of photoexcited holes is included in the “slip motion” model for photodarkening in the stage when the layer clusters are charged due to capture of charge carriers [14]. This model was used by us to explain the experimental results for amorphous As_2Se_3 films doped with tin [15]. Charge transport in chalcogenide glasses is known as highly dispersive due to wide distribution of capture times in multiple-trapping process. For glasses like a- As_2Se_3 the dispersive parameter β of hole transport is close to $\beta=0.5$, in accordance with the value found from

the stretched exponential presentation of photodarkening kinetics. In our case, for the composition $\text{As}_{45}\text{S}_{15}\text{Se}_{40}$, the value of the dispersion parameter was found $\beta=0.42$. The fact that β is increasing in the Se-rich compositions indicates to the increasing of the ordering in the structure of amorphous films. The composition dependence of photodarkening may be caused by the different ratio of homopolar chemical bonds (As-As, Se-Se) and heteropolar (As-Se) in investigated amorphous films, and which are responsible for the photodarkening [16,17].

4. Summary

The experimental investigations of the influence of the light irradiation and heat treatment on the optical parameters of one of highest sensitive chalcogenide glass $\text{As}_{45}\text{S}_{15}\text{Se}_{40}$ were investigated. It was found that for the amorphous $\text{As}_{45}\text{S}_{15}\text{Se}_{40}$ thin films the value of the refractive index n was found $n=2.921$ at $\lambda=650$ nm, increase with exposure time and decrease for the annealed samples. The optical band gap E_g determined from the Tauc plot $E_g=1.929$ eV decrease in both cases under the light exposure and heat treatment $\Delta E_g/\Delta T_{ann}=-5.8\cdot 10^{-4}$ eV/ $^\circ\text{C}$. The kinetics of photodarkening in amorphous $\text{As}_{45}\text{S}_{15}\text{Se}_{40}$ thin films is described by stretch exponential function and the effect at illumination with laser beam $\lambda=540$ nm is more pronounced that in amorphous As_2S_3 and As_2Se_3 films. The maximum of the diffraction efficiency η of the holographic gratings recorded during the exposure of laser beam at $\lambda=540$ nm is reached at about $t=250$ s.

The kinetics of photodarkening process in amorphous $\text{As}_{45}\text{S}_{15}\text{Se}_{40}$ thin films is described by stretched exponential function $T(t)/T(0) = A_0 + A \exp[-(t-t_0)/\tau]^{(1-\beta)}$, with the parameter $\beta \cong 0.42$.

Acknowledgement

The work is supported by the Institutional Project no. 11.817.05.03A.

References

- [1] J.Teteris, M.Reinfeld. J. Optoelectron. Adv. Mater. **5**(5), 1355 (2003).
- [2] A.Andriesh, M.Iovu.. Physica Status Solidi B **246**(8), 1862 (2009).
- [3] J.Teteris. J. Optoelectron. Adv. Mater. **4**(3), 687(2002).
- [4] M. S. Iovu, D. V. Harea, E. P. Colomeico, I. A. Cojocar. J. Optoelectron. Adv. Mater. **10**(12), 3469 (2008).
- [5] J. Teteris, M. Reinfeld. J. Optoelectron. Adv. Mater. **7**(5), 2581 (2005).
- [6] S. Onari, K. Asai, T. Arai. J. of Non-Cryst. Solids **76**(2-3), 243 (1985).

- [7] W. Li, S. Seal, C. Rivero et al. *J. of Applied Physics* **98**, 053503 (2005).
- [8] V. M. Rubish, V. O. Stefanovich, O. G. Guranich et al. *Ukr. J. Phys. Opt.* **8**(2), 69 (2007).
- [9] A. Ganjoo, R. Golovchak, *J. Optoelectron. Adv. Mater.*, **10**(6), 1328 (2008).
- [10] V. M. Lyubin *Non-Silver, Photographical Processes*, Edited by A.L.Kartujanskii, *Chimia, Leningrad*, pp. 193-215, 1984 (in Russian).
- [11] M. S. Iovu, V. G. Ciorba, E. P. Colomeico, M. A. Iovu, A. M. Nastase, A. Prisacari, M. Popescu, O. I. Shpotyuk. *J. Optoelectron. Adv. Mater.* **7**(5), 2333 (2005).
- [12] A. Gerbreders, J. Teteris. *J. Optoelectron. Adv. Mater.* **9**(10), 3164 (2007).
- [13] M. Kincl, K. Petkov, L. Tichy. *J. Optoelectron. Adv. Mater.* **8**(2), 780 (2006).
- [14] Shimakawa, N. Yoshida, A. Ganjoo, Y. Kuzukawa, J. Singh *J. Phil. Mag. Letters*, **77**(3), 153 (1998).
- [15] P. Boolchand, D. G. Georgiev, M. S. Iovu. *Chalcogenide Letters* **2**(4), 27-34 (2005).
- [16] M. Frumar, A. F. Firth, A. E. Owen. *J. of Non-Cryst. Solids* **59&60**, 921 (1983).
- [17] O. I. Shpotyuk. *Opto-Electronics Review* **11**(1), 19 (2003).

*Corresponding author: mihail.iovu@phys.asm.md